Tellus (1994), 46A, 351–366
Printed in Belgium – all rights reserved

TELLUS
ISSN 0280–6495

Climatology and variability in the ECHO coupled GCM

By M. LATIF*, T. STOCKDALE, J. WOLFF†, G. BURGERS‡, E. MAIER-REIMER, M. M. JUNGE, K. ARPE and L. BENGTSSON, *Max-Planck-Institut für Meteorologie, Bundesstraße 55, D-20146 Hamburg, Germany*

(Manuscript received 10 June 1993; in final form 14 March 1994)

ABSTRACT

ECHO is a new global coupled ocean-atmosphere general circulation model (GCM), consisting of the Hamburg version of the European Centre atmospheric GCM (ECHAM) and the Hamburg Primitive Equation ocean GCM (HOPE). We performed a 20-year integration with ECHO. Climate drift is significant, but typical annual mean errors in sea surface temperature (SST) do not exceed 2° in the open oceans. Near the boundaries, however, SST errors are considerably larger. The coupled model simulates an irregular ENSO cycle in the tropical Pacific, with spatial patterns similar to those observed. The variability, however, is somewhat weaker relative to observations. ECHO also simulates significant interannual variability in mid-latitudes. Consistent with observations, variability over the North Pacific can be partly attributed to remote forcing from the tropics. In contrast, the interannual variability over the North Atlantic appears to be generated locally.

1. Introduction

The development of complex coupled ocean-atmosphere general circulation models (GCMs) is a rapidly progressing field. Such sophisticated models can be categorized roughly into two classes: global coarse-resolution and limited domain high-resolution TOGA (Tropical Ocean Global Atmosphere) models. The term "limited domain high-resolution" refers generally to the oceanic component in the latter class of models. The global coarse-resolution coupled models were generally designed to address the global change problem (Washington and Meehl, 1989; Manabe et al., 1990; Murphy, 1990; Cubasch et al., 1992). The global coupled models have been also useful in gaining some insight into the nature of natural climate variability (e.g., Meehl, 1990; Lau et al., 1992; Delworth et al., 1993), and long integrations were performed with such models to estimate the natural climate variability spectrum against which a potential anthropogenic climatic signal can be detected. However, their ability to simulate natural climate variability is limited to some extent by the coarse resolution. The tropical problem of air–sea interaction, for instance, has shown that higher resolution is required to simulate a realistic El Niño/Southern Oscillation (ENSO) (e.g., Neelin et al., 1992; Lau et al., 1992; Philander et al., 1992).

The limited domain TOGA models were developed to investigate specifically the dynamics and predictability of the ENSO phenomenon (e.g., Gordon, 1989; Philander et al., 1992; Nagai et al., 1992; Latif et al., 1993a, b). They consist of a high-resolution tropical ocean GCM which is coupled to a coarse-resolution global atmospheric GCM. Such models simulate realistically the ENSO variability and show some skill in predicting ENSO-related climate anomalies. The TOGA models, however, are inherently limited in their

* Corresponding author.
† Present affiliation: Antarctic CRC, University of Tasmania, GPO Box 252C, Hobart, Tasmania 7001, Australia.
‡ Permanent affiliation: KNMI, Postbus 201, 3730 AE de Bilt, The Netherlands.

applicability to tropical air–sea interactions and their impact on the global atmospheric circulation. Thus, in order to get more insight into the nature of natural climate variability on a global scale, global high-resolution coupled GCMs are desirable.

Such models are currently developed at several institutions worldwide. In this paper, we present such a coupled GCM which was integrated for twenty years. We like to emphasize, however, that the most suitable methodology to increase our present understanding of climate variability should involve a hierarchy of models, ranging from simple and intermediate models to complex GCMs, and the simultaneous analysis of data. We are therefore also developing simpler models to explore more systematically the possible behaviours in different regions of the parameter space.

The intention behind the development of a global high-resolution coupled GCM is threefold. First, we would like to explore the dynamics of the annual cycle globally. Second, we would like to use the model to investigate the dynamics of interannual and decadal-scale variability, and third, we would like to explore systematically the predictability of these fluctuations. Here, we concentrate of the first two aspects. The issue of climate predictability will be addressed in a forthcoming paper. We do not make use of flux correction (Sausen et al., 1988) in order to faciliate the diagnosis of problems in the individual model components which lead to climate drift of the coupled system. These deficiencies are not always obvious when the models are run in the uncoupled mode, and we tried to reduce some of these problems by tuning the coupled system. At this stage of the model development, however, we have not included a sea-ice model. Ocean and atmosphere interact therefore within the region 60°N to 60°S only which is in some sense equivalent to the application of flux correction, but probably less stringent.

This paper is organized as follows. We describe the coupled GCM in Section 2. Section 3 deals with the tuning of the upper ocean mixing parameterization running the model in the coupled mode. The simulation of the tropical climatology and variability is described in Section 4, while the coupled model's performance in mid-latitudes is presented in Section 5. We conclude the paper in Section 6.

2. Coupled model

The atmospheric component of our coupled GCM "ECHO" is ECHAM, the Hamburg version of the European Centre operational weather forcasting model. The formulation of the dynamical part still resembles the one in the European Centre version, while the parameterizations of subgrid scale processes were mainly developed in Hamburg. The model is described in detail in two reports (Roeckner et al., 1992; DKRZ, 1992). ECHAM is a global low-order spectral model with a triangular truncation at wavenumber 42 (T42). The nonlinear terms and the parameterized physical processes are calculated on a 128×64 Gaussian grid which yields a horizontal resolution of about $2.8° \times 2.8°$. There are 19 levels in the vertical which are defined on σ-surfaces in the lower troposhere and on p-surfaces in the upper troposphere and in the stratosphere. The model includes standard physics (for details the reader is referred to Roeckner et al., 1992). Earlier versions of ECHAM have been applied in various climate simulations and response experiments which are summarized in two reports (Fischer, 1987; Von Storch, 1988). The low-frequency behaviour of these earlier versions when forced by observed sea surface temperatures (SSTs) is described by Latif et al. (1990) and Barnett et al. (1991). The current version of ECHAM which we use here was integrated as part of AMIP (Atmospheric Model Intercomparison Project). Some preliminary results of this AMIP run are given in Arpe et al. (1992).

The ocean model is "HOPE" (Hamburg Ocean Model in Primitive Equations) which is based on primitive equations simplified by making use of the hydrostatic and Boussinesq approximations. The HOPE model is a further development of the models used by Latif (1987), Barnett et al. (1991), Luksch and Von Storch (1992), and Latif et al. (1993a, b). Its domain is global and we use realistic bottom topography. Active salinity is included in HOPE. The meridional resolution is variable, with 0.5° within the region 10°N to 10°S. The resolution decreases poleward to match the T42-resolution of the atmosphere model. The zonal resolution is constant and also matches the atmospheric model resolution. Vertically, there are 20 irregularly spaced levels, with ten levels within the upper 300 m. Since we have not yet included a sea-ice model in HOPE, the SSTs and sea surface

salinities are relaxed to Levitus, 1982 climatology poleward of 60°, using Newtonian formulations with time constants of about 2 and 40 days, respectively for the upper layer thickness of 20 m.

The two models were coupled without applying flux correction. They interact over all 3 oceans in the region 60°N–60°S. The ocean model is forced by the surface wind stress, the heat flux, and the freshwater flux simulated by the atmosphere model, which in turn is forced by the SST simulated by the ocean model. The coupling is synchronous, with an exchange of information every two hours. The coupled GCM is forced by seasonally varying insolation. The oceanic initial conditions are those simulated at the end of a 15-year integration with climatological forcing. Since we are mainly interested in the variability of the upper ocean, this relatively short spin up time is justified. The atmospheric initial conditions are taken from a control run with climatological SST. The coupled integration is started at 1 January and continued for 20 years.

3. Tuning of the ocean surface mixing physics

If a coupled GCM is to be run with no flux correction or other constraints, perhaps the most important aspect of model performance is the ocean surface heat balance. This depends on both the surface fluxes from the atmosphere model and the mixing of heat in the surface layers of the ocean. We consider here the sensitivity of the ocean surface heat balance to the ocean mixing. The HOPE ocean model has three main processes that affect the surface mixing of heat. These are a Richardson number dependent mixing scheme, a surface mixed layer parameterization, and the penetration of solar radiation beneath the ocean surface.

The Richardson number scheme determines vertical viscosity ν and diffusivity κ according to the formulae:

$$\nu = A_0/(1 + (5\,\mathrm{Ri})^2) + \nu_b \tag{1}$$

$$\kappa = D_0/(1 + (5\,\mathrm{Ri})^2) \tag{2}$$

where typical values are $A_0 = 4 \cdot 10^{-3}\ \mathrm{m^2/s}$, $D_0 = 2 \cdot 10^{-3}\ \mathrm{m^2/s}$, $\nu_b = 1 \cdot 10^{-6}\ \mathrm{m^2/s}$, and Ri is the Richardson number defined by:

$$\mathrm{Ri} = -g\rho_z/((u_z)^2 + (v_z)^2). \tag{3}$$

The density and horizontal current components are given by ρ, u, and v, respectively. Subscripts denote derivatives in (3).

The surface mixed layer parameterization is partially diagnostic and very simple. The depth of the mixed layer is diagnosed according to the temperature difference between any given layer and the surface: if this difference is less than a specified critical value ΔT_c, the layer concerned is considered to be part of the surface mixed layer. The turbulent mixing within the mixed layer is parameterized by adding a fixed vertical diffusivity/viscosity to the Richardson number dependent mixing given by (1) and (2). Levels beneath the diagnosed mixed layer have no turbulent mixing added.

Mathematically,

$$\begin{aligned} \nu_{ML} = \kappa_{ML} &= W_0, \qquad \text{for} \quad (T - T_0) \leqslant \Delta T_c \\ &= 0, \qquad \text{for} \quad (T - T_0) > \Delta T_c, \end{aligned} \tag{4}$$

where T_0 is the surface temperature, and typical values of the constants are $W_0 = 2 \cdot 10^{-3}\ \mathrm{m^2/s}$ and $\Delta T_c = 0.5°\mathrm{C}$.

Penetration of solar radiation beneath the ocean surface is included in the model physics, and this also has an effect on the mixing of the surface layers. The transmission of sunlight is calculated using a two-stream approximation, with long and short wavelengths absorbed rapidly, and intermediate wavelengths being attenuated exponentially with depth. The coefficients used should ideally be functions of solar elevation, cloud cover and water type; instead average values are used that are appropriate for clear mid-ocean water in typical conditions, using data from Paulson and Simpson (1977) for guidance. The fraction absorbed rapidly is 0.6, and it is assumed that all of this energy is absorbed in the first model layer (a typical exponential fit would give a length scale of 1 m, very much smaller than the 20-m surface layer depth). The penetrating component has an exponential depth of 20 m. In total about 15% of the surface solar radiation penetrates beneath the surface layer of the model.

The initial set of parameter choices was to use a deep surface mixing ($\Delta T_c = 1.0°\mathrm{C}$), no solar penetration, and a shear dependent mixing with only weak mixing of heat ($A_0 = 4 \cdot 10^{-3}\ \mathrm{m^2/s}$, $D_0 = 2 \cdot 10^{-4}\ \mathrm{m^2/s}$). These values had been found to give good results in simulating the mean

seasonal cycle of the ocean when the model was forced with monthly mean climatological fluxes. SST errors were typically less than 0.5°C and heat flux errors less than 25 W/m^2 in most regions of the tropical Pacific in this uncoupled ocean model run, and the thermocline at the bottom of the western Pacific warm pool was better defined relative to earlier studies without a mixed layer parameterization.

Although the behaviour of the coupled model with these mixing parameters was reasonable, three issues caused concern. Firstly, the seasonal cycle of SST in the East Pacific was slightly too weak in amplitude and showed a warming as early as September, rather than December/January as is observed. Secondly, the interannual SST variability as simulated by the ocean model when forced by observed wind stresses was much too small. Probably, this was related to the too deep thermocline in the East Pacific. Thirdly, the annual summer warming in the mid-latitudinal SST of the northern hemisphere was much too weak. Therefore several other combinations of mixing parameters were tried (Table 1), partly to see if the original formulation could be improved upon, and partly to explore the sensitivity of the coupled system to changes in surface mixing.

We removed the surface mixing term altogether in a first sensitivity experiment (experiment 2), and as a partial compensation increased the shear dependent diffusivity D_0 from 2 to 20 cm^2/s (surface winds are able to produce considerable surface mixing in the presence of a large enough shear-dependent term, and many well-proven tropical ocean models rely on this process). The solar penetration was also removed in this first sensitivity experiment. The impact on the coupled system of these changes was surprisingly large,

Table 1. *Experiments performed to investigate the sensitivity of the coupled system to the parameterization of surface mixing processes*

No.	Duration	Add. mixed layer mixing	Sol. pen.	D_0 (cm^2/s)
1	40 mo	yes, $W_0 = 20$ cm^2/s, $\Delta T_c = 1.0$°C	yes	2
2	2 mo	no	no	20
3	2 mo	no	yes	20
4	20 yrs	yes, $W_0 = 20$ cm^2/s, $\Delta T_c = 0.5$°C	yes	20

with warm SSTs spreading rapidly from the west Pacific across the whole equatorial basin, causing the southeast trades to weaken and the whole coupled ocean-atmosphere system to move to an unrealistic "warm" state within a relatively short time. SSTs in the east at 10°S were substantially warmer than is seen in any El Niño event, and were therefore judged as definitely unrealistic. We terminated this run after 2 months.

A 3rd experiment was made using the same mixing parameterizations, but reintroducing solar penetration. This has a similar effect to an increase in surface mixing, and might be expected to cool SST, especially in regions where the warm surface layer is very shallow, as was the case for our "overheated" eastern Pacific. Sure enough, the solar penetration slowed and significantly reduced the overheating. This, however, was not enough to prevent the warming and the consequent coupled effects. We therefore terminated this run also after two months.

A 4th experiment kept the solar penetration and the increased shear dependent mixing, but reintroduced the surface mixing term. The value of ΔT_c, however, was set to 0.5°C, a more realistic figure in view of the physical motivation of the scheme. (This parameter setting enhanced the interannual variability in the uncoupled ocean model run with observed wind stresses and improved considerably the thermocline structure in the east Pacific. The SST and heat flux errors, however, were about twice as large as in the first experiment.) The SSTs simulated in the coupled mode remained under control once more, and a warm, shallow, highly stratified mixed layer did not occupy the tropics. The overall simulation was not in fact very different from the first experiment. The amplitude of the east Pacific seasonal cycle in SST was enhanced, but the phase problems were basically unchanged. The summer warming in the mid-latitudes of the northern hemisphere was more pronounced, but still too weak. Overall (considering both the results of the limited experimentation and theoretical preferences), this fourth simulation was felt to be an improvement on the first, and in fact forms the basis for the rest of this paper.

To summarize these results, it is clear that on the one hand a coupled GCM can be very sensitive to relatively small changes in surface mixing (e.g., experiments 2, 3), and on the other, significant

differences in mixing do not always have much impact on the mean state (experiments 1, 4). The cause of the sensitivity seen in some of these experiments seems to be feedbacks between warm SST, increased surface stratification and reduced surface mixing, and reduced wind speeds and evaporation. If the system is in a regime where these feedbacks are acting strongly, then it is very sensitive to any changes in the surface heat balance.

Fortunately, the real ocean-atmosphere system seems not to be in such a sensitive regime. The sizeable interannual variability associated with ENSO does not trigger run-away "surface warming" events of this sort. It is also gratifying that our two realistic simulations (experiments 1, 4) also show little sensitivity to these feedback processes. The conclusion must be that for a sufficiently realistic model, the mean state is not hyper-sensitive to the ocean surface mixing. Perhaps we can hope that this is a general property of the ocean-atmosphere climate system: coupled interactions can lead to large errors if the models contain errors above certain threshholds, but these large coupled errors can disappear once a model system is brought into the correct climatic regime.

4. Tropical performance

4.1. Climatology

The coupled model undergoes considerable climate drift (Fig. 1). The annual mean SST errors (relative to Reynolds', 1988 climatology) computed from all 20 years are largest near the eastern boundaries of the tropical oceans which are simulated much too warm (Fig. 1). The largest errors are found in the Southern Hemisphere in the region 10°S–20°S, attaining maximum values of about 4°C in the Pacific and 6°C in the Atlantic Ocean in the immediate vicinity of the coasts. The tongue of positive SST errors has a zonal extension of about 30°. The larger part of these errors result from the first ten years of the integration (Fig. 2a). A similar error pattern is found in the Northern Hemisphere, but with considerably smaller SST errors. The western Pacific and the Indian Ocean SSTs are simulated at about the correct temperatures within about ± 1°C.

The SST in the eastern equatorial Pacific, as expressed by the Niño-3 index (5°N–5°S, 150°W–90°W), shows a gradual cooling during the first 15 years, after a relatively strong initial rise (Fig. 2a). The Niño-3 SST is rather stable during the last five years of the integration. It is not clear after the twenty years of integration, which fraction of the cooling can be attributed to climate drift of the coupled system, and which fraction is related to interdecadal variability. The same is true for the SST in the western equatorial Pacific (Fig. 2b) which shows some rise of SST in the Niño-4 region (5°N–5°S, 160°E–150°W) at the end of the integration, after a relatively long cooling phase.

The reason for the failure of the coupled model in the eastern tropical oceans is propably related to the inability of our atmospheric GCM to simulate sufficient low-level stratus clouds in these regions, leading to an excess of incoming solar radiation at the sea surface. Observational estimates of cloud cover are of the order of 70 to 80% over the southeastern tropical oceans (Oberhuber, 1988a). The cloud cover in the coupled model attains typical values of 30% only. Thus, the annual mean incoming solar radiation is much larger in the coupled run, attaining values of about 250 W/m^2, while Oberhuber's, 1988b climatology indicates values of about 150 W/m^2. Additionally, the coarse zonal resolution of the ocean model (~ 2.8°) is not adequate to resolve the narrow coastal upwelling zones which might enhance the problem.

The problems with the low-level stratus clouds influence also the coupled model's performance of the annual cycle in the eastern equatorial Pacific. Consistent with observations, the coupled model does simulate a pronounced annual cycle, although there is almost no annual cycle forcing at the equator. However, as can be seen from the time series of the Niño-3 SST (Fig. 2a), the coupled model's annual cycle shows significant differences to the observed one. While the spring warming and the following drop in SST are simulated reasonably well, the ocean warms again around September, in contrast to the observations which show the warming not before December. Overall, the coupled model tends to overestimate the semi-annual cycle. This behaviour suggests that the errors in the solar radiative flux have a significant impact on the simulated annual cycle. This view is also supported by the results of Stockdale et al. (1994). They coupled an identical version of

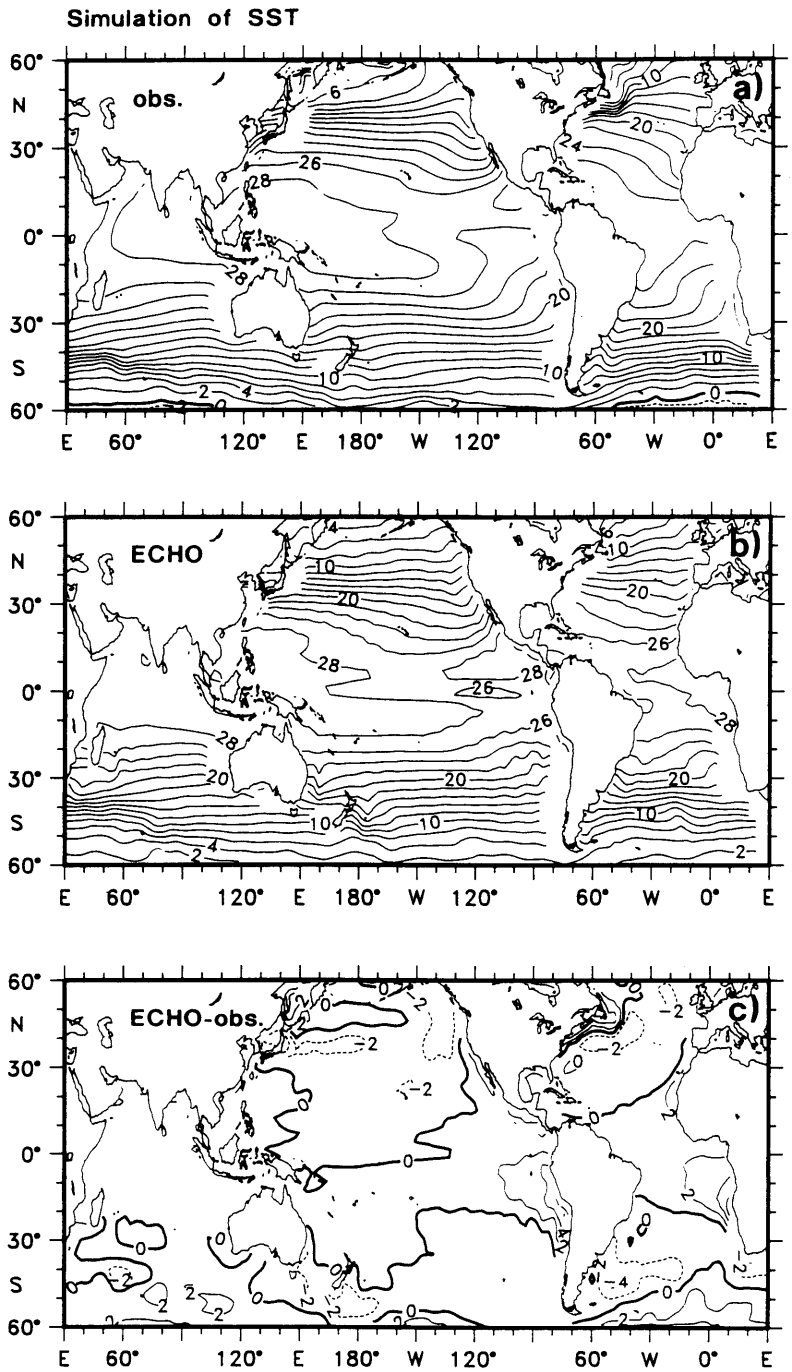

Fig. 1. (a) Annual mean SST derived from the Reynolds, 1988 data set, (b) annual mean SST derived from the 20-year coupled run, and (c) difference between the coupled model and the Reynolds climatology. The contour interval is 2°C in all 3 panels.

the HOPE ocean model to the European Centre atmosphere model, tuned its diagnostic cloud parameterization to yield an increased cloud amount over the eastern tropical oceans, and obtained a more realistic simulation of the annual cycle in Niño-3 SST. Such a tuning is not easily possible in our ECHAM atmosphere model, because our cloud scheme is formulated prognostically.

The observations indicate that the SST climatology in the western equatorial Pacific is characterized by a substantial semi-annual cycle in addition to the annual cycle (Fig. 2b). The coupled model captures this behaviour, but the changes associated with the annual and semi-annual cycles are stronger than observed. The reason for this model failure can be traced back to the warm pool structure which is simulated too shallow relative to observations. The model western Pacific warm pool extends to a depth of about 80 m only (not shown), while observational estimates indicate a depth of at least 120 m (Gill, 1982). This leads to a too strong sensitivity to surface forcing. Further sensitivity studies are needed with our coupled model to explore the origin of this model failure.

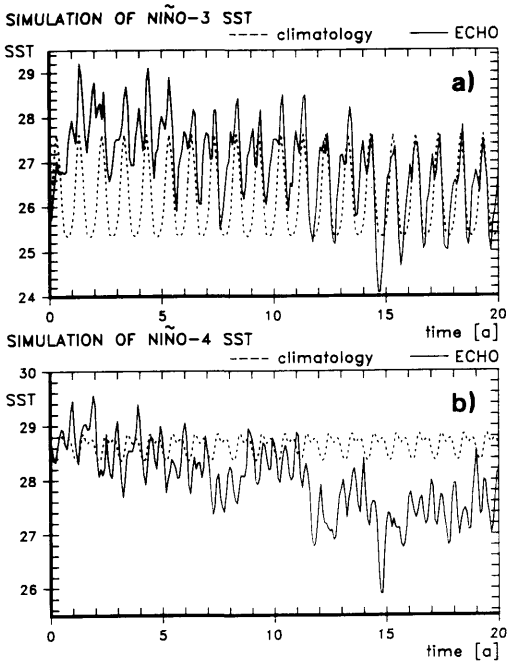

Fig. 2. (a) Niño-3 SST (a) and Niño-4 SST (b) as simulated by the coupled model (solid lines). The corresponding Reynolds climatologies are given for reference and repeated year by year (dashed lines).

Another rather sensitive parameter in general circulation models is rainfall. Here we compare the coupled model's rainfall climatology (Fig. 3d) with two observational estimates (Legates and Willmott, 1990; Jäger, 1976) (Figs. 3a, b) and with that obtained in an uncoupled control integration with the ECHAM atmosphere model forced by climatological SST (Fig. 3c). We use both available climatologies in this comparison to provide some indication of the uncertainty in observational rainfall estimates. The coupled model's rainfall climatology is generally in reasonable agreement with the observations. Over the western equatorial Pacific, however, the coupled model does not simulate enough rainfall. This tendency is already seen in the uncoupled control run with the ECHAM model, but significantly enhanced by the coupling. The reason for the further reduction in rainfall over the western Pacific is the slightly too cold SST in the coupled run (Fig. 2b). The tendency of the ECHAM model to simulate a split ITCZ (Intertropical Convergence Zone) over the Pacific is also enhanced by the coupling. This deficiency is also related to errors in SST which is simulated too zonal by the coupled model (Fig. 1).

In summarizing the results of this section, the coupled model's tropical climatology shows considerable deficiencies, especially in the eastern tropical oceans. Nevertheless, since no flux correction was applied and errors considerably larger than 1 °C are limited to relatively "small" regions (Fig. 1), the coupled model did a reasonable job in reproducing the tropical climatology.

4.2. Interannual variability

The coupled GCM simulates significant interannual variability in the Pacific which is rather irregular. As expected, the time series of the anomalous Niño-3 SST and Southern Oscillation Index (SOI) fluctuate coherently out phase on interannual time scales (Fig. 4) which visualizes the coupled nature of the interannual variability. The spatial patterns of the anomalies associated with the simulated interannual variability are in many respects similar to those observed during extremes of the ENSO cycle (Fig. 6). The meridional extent of the SST anomalies, however,

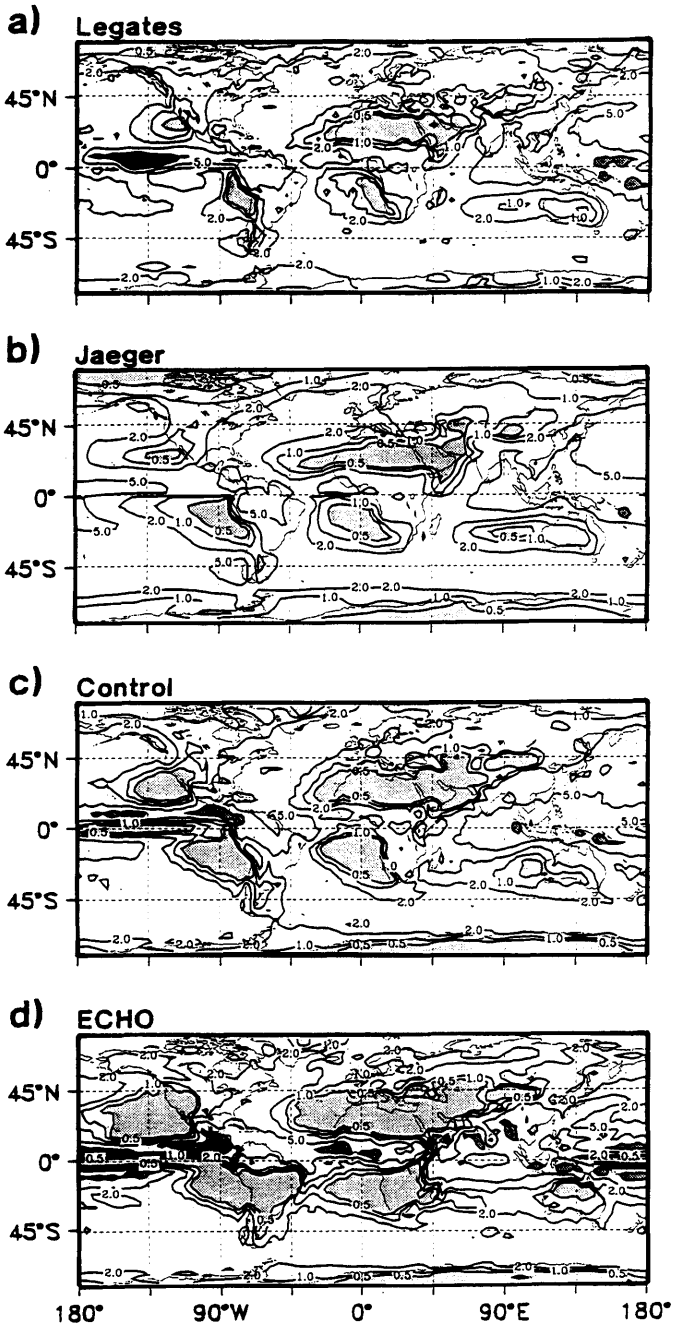

Fig. 3. (a) Annual mean rainfall derived from the Legates and Willmott (1990) climatology, (b) annual mean rainfall derived from the Jäger (1976) climatology, (c) annual mean rainfall derived from an uncoupled run with the atmosphere model forced by climatological SSTs, and (d) annual mean rainfall derived from the 20-year coupled model run. Contours shown are: 0.5 mm/d, 1 mm/d, 2 mm/d, 5 mm/d, and 10 mm/d. Light stippling indicates rainfall of 0.5 mm/d and less, while heavy stippling indicates rainfall of 10 mm/d and more.

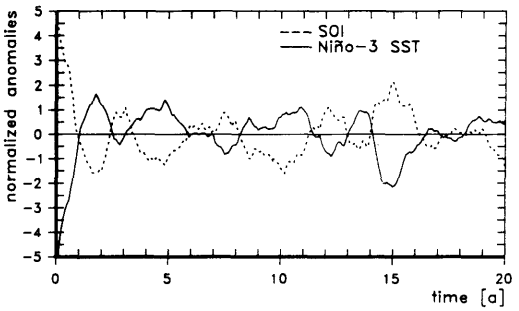

Fig. 4. Time series of the simulated anomalous Niño-3 SST anomalies (full line) and Southern Oscillation Index (SOI) (dashed line). The time series were detrended and normalized by their corresponding standard deviation, and a 13-months running mean was applied.

is underestimated by the model (Fig. 5). Thus, maximum SST anomalies averaged over the Niño-3 region attain values of about 1°C only, while observations indicate variations which are at least twice as large. At the equator, the simulated SST anomalies are only slightly smaller than the observed anomalies (Fig. 5). However, we would like to note that the observed SST anomalies also exhibit pronounced interdecadal variations. If we compare the observed variability during the period 1950–1979 (as shown in the atlas of Shea, 1986) with that observed during the period 1970–1990 (Fig. 5a), considerable differences are apparent, and the model variability is more consistent with the results of Shea, 1986. Thus, a longer run with

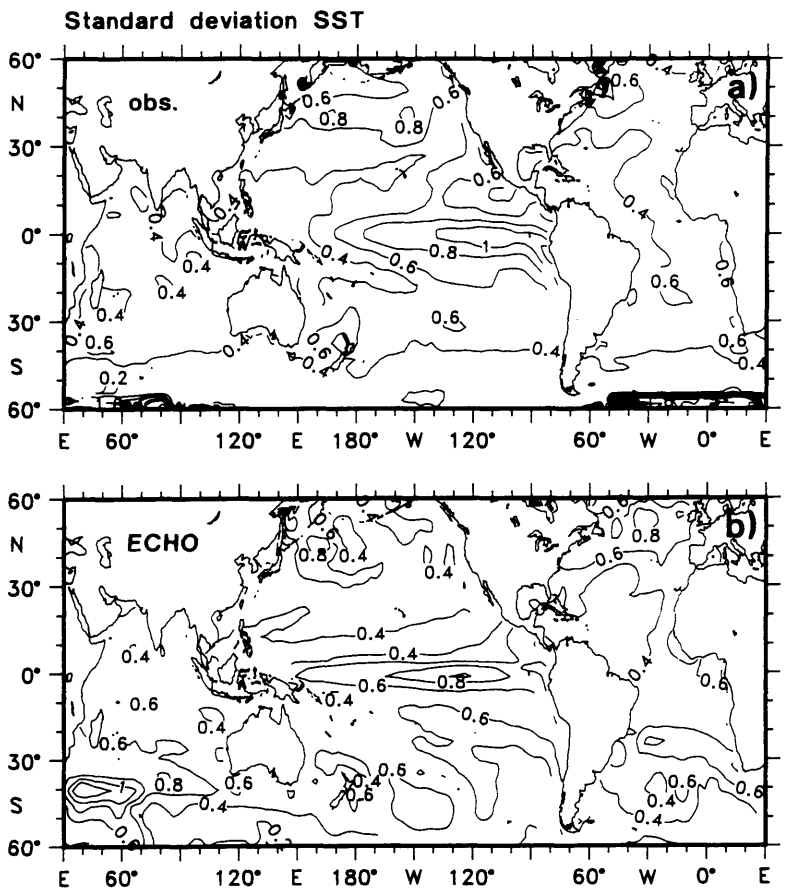

Fig. 5. (a) Standard deviation of monthly SST anomalies computed from the period 1970–1990 from the Reynolds data set, (b) standard deviation of monthly SST anomalies computed from years 2 to 20 of the coupled integration. The linear trend was removed prior to the analysis. Units are in (°C) in both panels.

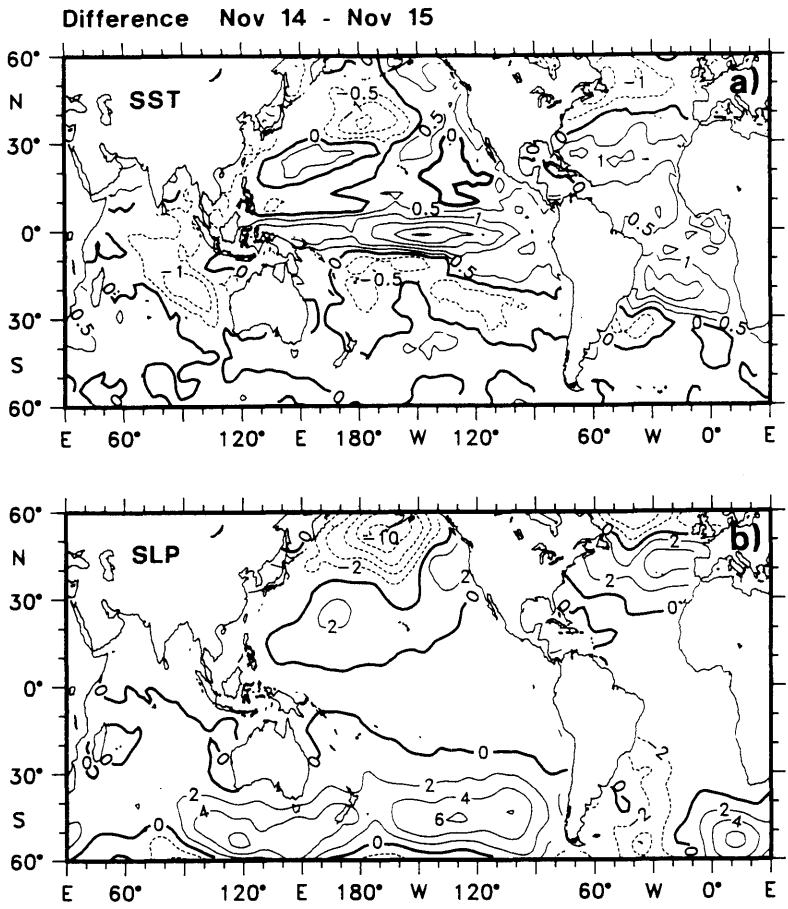

Fig. 6. (a) Difference in SST between Novembers, years 14 and 15. Temperature differences are given in (°C). (b) Same as in (a) but for sea level pressure. Pressure differences are in (hPa). Band-pass filtering (retaining variations with periods between 1 and 10 years) was applied prior to the analysis.

our coupled model is needed, in order to estimate the full spectrum of the model variability.

The mechanism for the ENSO-like variability in the model is at least partly related to the subsurface memory of the coupled system. As in the earlier version of our coupled model (Latif et al., 1993a, b) and consistent with the "delayed action oscillator" scenario (Schopf and Suarez, 1988), SST and zonal wind anomalies evolve in place, while upper ocean heat content adjusts slowly to previous changes in the surface wind stress field (not shown). If the "delayed action oscillator" operates in our coupled model, the ENSO-related variability would exhibit a preferred time scale. The spectrum of Niño-3 SST anomalies, however, shows an only marginally significant peak at a period of about three years (not shown), which suggests that stochastic forcing by the atmosphere is also important in generating oceanic low-frequency variability. Our coupled run, however, is too short to make precise statements about the relative roles of deterministic and stochastic processes. Therefore, we are presently continuing the coupled integration.

In order to obtain an indication of the spatial structure of the simulated interannual variability, we computed the difference in (band-pass filtered) SST and sea level pressure (SLP) between Novembers of years 14 and 15 (Fig. 6). This time interval is the most active period, characterized by a fast

transition from an anomalously warm (year 14) to an anomalously cold phase (year 15). We chose this particular period because one can expect global impacts of tropical Pacific SST anomalies to be strongest during such extreme phases. The Pacific is characterized by a strong positive SST anomaly centered at the equator near 130°W (Fig. 6a). This "El Niño" SST anomaly is surrounded by predominantly negative SST anomalies. The coupled model simulates a strong negative SST anomaly in the North Pacific, a feature which is consistent with observations and described previously in many studies (e.g., Weare et al., 1976). We return to this point below when discussing the interannual variability in mid-latitudes.

5. Mid-latitudinal performance

5.1. Climatology

Climate drift is appreciably small, and, in the case of the North Atlantic, not clearly separable from interdecadal variability (Fig. 7). The performance of ECHO in mid-latitudes is characterized by too cold SSTs in most regions (Fig. 1). Typical SST errors are of the order of −2°C, touching −4°C in very small regions. Too warm SSTs are simulated in localized regions near the western boundaries in the Northern Hemisphere. The phase of the annual cycle is simulated well by the coupled model, as visualized by three examples, the North Pacific, North Atlantic, and South Indian Ocean SST (Fig. 7). The amplitude of the annual cycle in the northern hemisphere is significantly understimated by the model. The reason for the too weak annual cycle is probably related to an excess of mixing in the ocean, prohibiting the formation of a shallow mixed layer in summer, leading to too cold temperatures. Consistent with this picture, largest SST errors are found in northern summer.

We would like to note one further interesting feature. It appears that the coupled model is more successful in simulating the mean SST in certain regions than the ocean model alone when run in the uncoupled mode with prescribed boundary conditions. This is particularly obvious in mid-latitudes, especially in the Southern Ocean (Fig. 7c). The reason for this unexpected result is that accurate surface heat flux estimates are necessary to obtain a realistic climatology in mid-

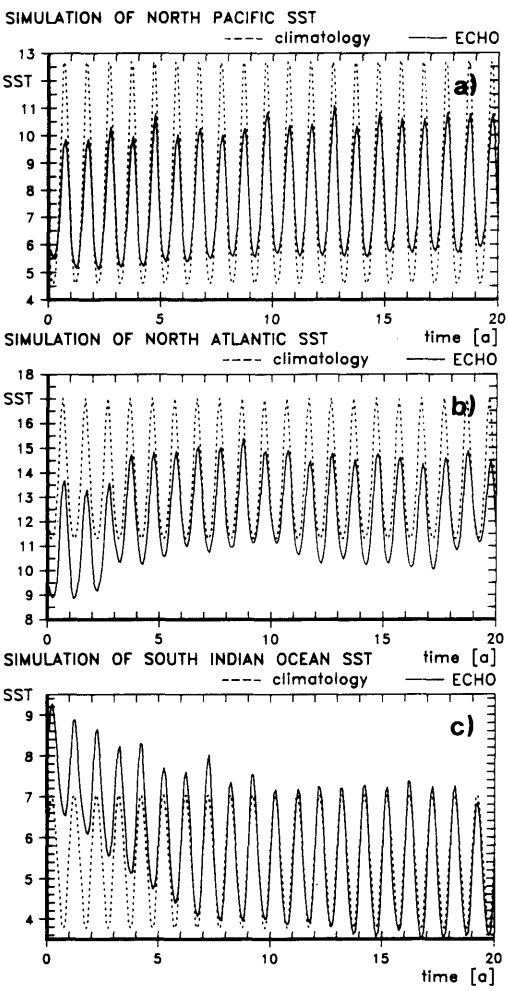

Fig. 7. (a) North Pacific (40°N–60°N, 160°E–160°W) SST as simulated by the coupled model. (b) Same as (a) but for the North Atlantic (40°N–60°N, 40°W–10°W). (c) Same as (a) but for the Southern Indian Ocean (40°S–60°S, 20°E–60°E). The solid lines denote the model SSTs. The corresponding Reynolds climatologies are given for reference and repeated year by year (dashed lines).

latitudes in uncoupled ocean model simulations. Since surface heat flux estimates derived from observations are due to large uncertainties or not even available, as over large regions of the Southern Oceans, it is not surprising that our uncoupled simulation exhibited relatively large SST errors in these regions. These errors, however, can be reduced significantly in a coupled integra-

tion, provided both individual model components are sufficiently realistic.

5.2. Interannual variability

We shall not address the question of decadal-scale fluctuations which are obvious in the area-averaged time series of north Atlantic SST (Fig. 7b). These fluctuations will be discussed in a forthcoming paper describing the results of a multi-decadal run with ECHO. The level of inter-annual variability in mid-latitudes is simulated correctly in most regions by the coupled GCM. Standard deviations of SSTs in the North Atlantic and Pacific are simulated at about 0.5°C (Fig. 5b) which is in good agreement with observations (Fig. 5a). Part of the variability in the North Pacific is forced remotely by the tropics (Fig. 6a). As described by Alexander (1990) and Luksch

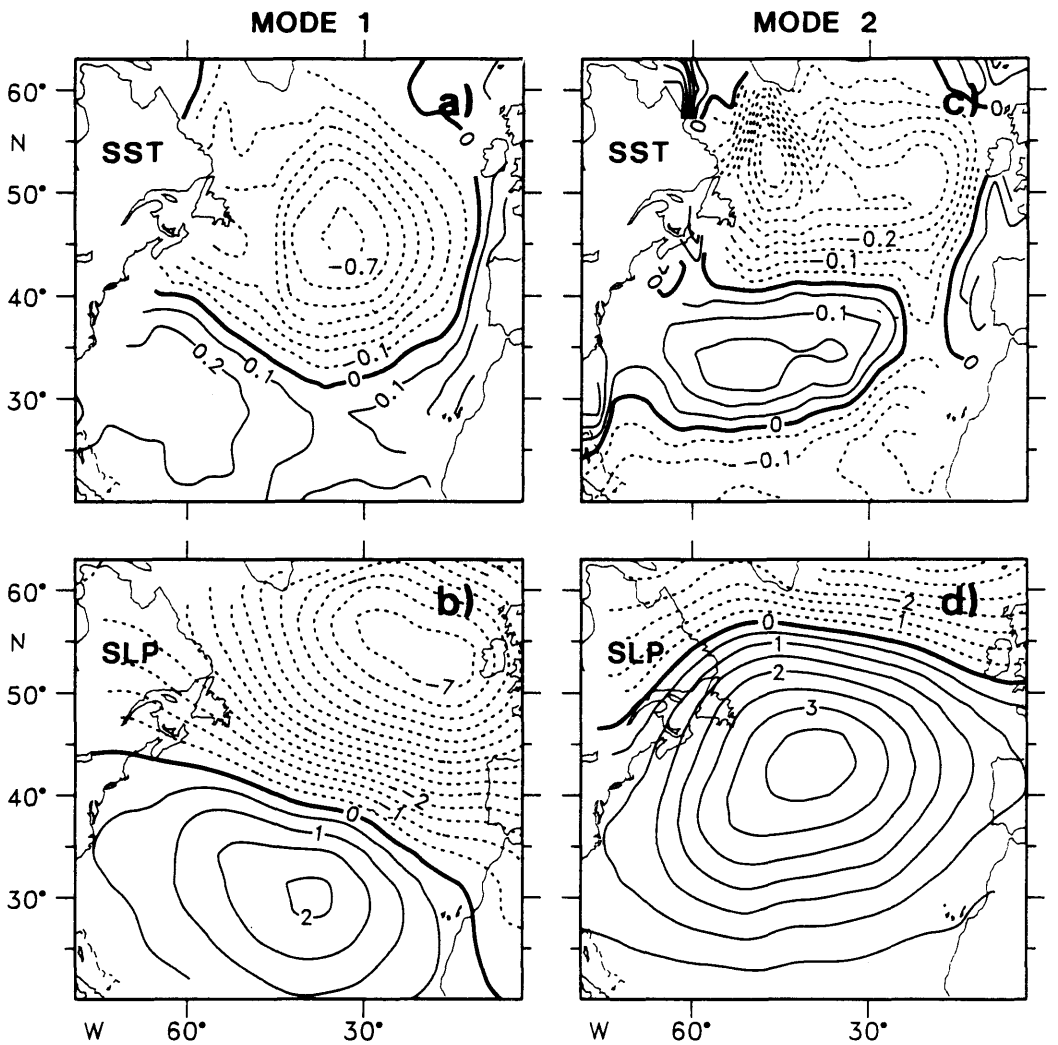

Fig. 8. First 2 leading CCA modes of North Atlantic SST and SLP as simulated by the coupled model. (a) Canonical predictor (SST) pattern (°C) of the leading CCA mode, (b) canonical predictand (SLP) pattern (hPa) of the leading CCA mode, (c) canonical predictor (SST) pattern (°C) of the second CCA mode, (d) canonical predictand (SLP) pattern (hPa) of the second CCA mode. The values correspond to a one standard deviation change.

and Von Storch (1992), for instance, positive equatorial Pacific SST anomalies force an intensified Aleution low which leads to anomalously strong cold air advection over the western and central north Pacific forcing the negative SST anomalies observed. This mechanism operates also in our coupled model (Fig. 6b). However, the ENSO-related variability accounts for about only 10% of the total SST variance in the north Pacific, and the correlations between North Pacific SST and Niño-3 SST are only maginally significant. In Fig. 6a, there are also found SST anomalies in the other oceans, but correlations of SST anomalies in these regions with Niño-3 SST anomalies are well below the significance limits, suggesting that these anomalies are of independent origin.

In order to get an impression of the spatial scales involved in the simulated north Atlantic interannual variability, we performed a canonical correlation analysis (CCA) of north Atlantic SST and SLP anomalies. We restricted the CCA to the winter months only (December, January, February). We retained the leading 5 empirical orthogonal functions (EOFs) only in the CCA, explaining about 85% of the variance in each field. The leading CCA mode from the coupled model attains a canonical correlation of 0.65 and explains 21% of the variance of the SST and 43% of the variance of the SLP data. Both the canonical predictor (SST) and predictand (SLP) patterns show a dipole structure (Figs. 8a, b) and are very similar to the patterns of the leading CCA mode derived from observations (Zorita et al., 1992). The SST pattern (Fig. 8a) shows mostly negative values between 40° N and 60° N, with a maximum near 45° N and 30° W. Positive anomalies are found south of this region, with strongest anomalies off the coast of North America. Local explained variances in SST amount to about 70% in the centre of the negative region and 40% in the positive region. The corresponding canonical SLP pattern (Fig. 8b) exhibits extremes near 55° N and 25° W and near 30° N and 40° W. Local explained variances in these centres of action amount to 90% and 40°%, respectively.

The next CCA mode has a canonical correlation of 0.53, explaining 7% in the SST and 18% in the SLP data. This mode is similar to the 2nd CCA mode derived from the SST and SLP observations (Zorita et al., 1992). The canonical SST and SLP patterns are also characterized by dipole structures and shifted northward relative to those of the leading CCA mode. The canonical SST pattern (Fig. 8c) exhibits a negative extreme near 55° N and 50° W and a positive extreme near 35° N and 55° W. The local explained variances in these centers of action amount to 50% and 25%, respectively. The canonical SLP pattern (Fig. 8d) of the 2nd mode shows a maximum near 45° N and 40° W and negative values north of 55° N which intensify poleward. Local explained variances in the high pressure center amount to about 75%, while those in the low-pressure region attain values up to about 30%.

The results of our CCA analysis are consistent with the picture that the atmosphere drives the ocean. Both shown canonical SLP patterns reflect

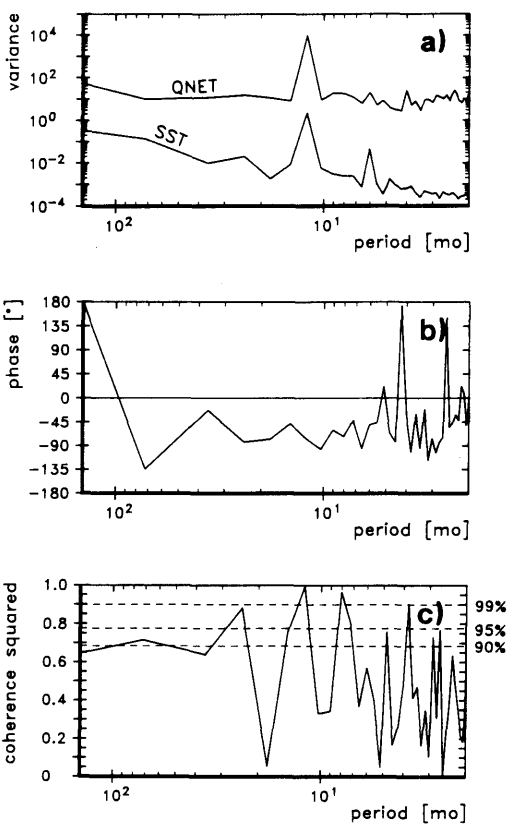

Fig. 9. (a) Autospectra of North Atlantic SST (shown in Fig. 7b) and net surface heat flux. (b) Phase spectrum and (c) coherence spectrum between the two time series. The bandwith used is 72 months which yields 6 degrees of freedom.

internal modes of the atmosphere, as decribed in many papers (Wallace and Gutzler, 1981; Barnston and Livezey, 1987). The SLP pattern of the leading CCA mode (Fig. 8b) is often referred to as the "east Atlantic" mode and that of the second CCA mode (Fig. 8d) to as the "North Atlantic Oscillation". Our atmosphere model is able to reproduce these variability modes (Zoriata et al., 1992), and the ocean model responds passively to the associated variations in the surface heat and momentum fluxes, as shown by Luksch (personal communication). For a more detailed discussion of this issue, see, for instance, Zorita et al. (1992) and references herein.

Thus, our results are consistent with the Hasselmann (1976) stochastic climate model scenario. Autospectra of north Atlantic SST indices are red, while typical atmospheric indices are characterized by white spectra. A typical example is shown in Fig. 9a, which shows the spectra of area-averaged North Atlantic SST (Fig. 7b) and net surface heat flux. Also shown is a cross spectral analysis of the two time series (Figs. 9b, c). Both time series exhibit highly significant peaks at the annual frequency. The cross spectral analysis suggests that the atmosphere forces the ocean at annual and interannual time scales. Both time series are coherent at these time scales, and, consistent with the observational work by Cayan (1992), the SST lags the heat flux. Such behaviour is expected according to the Hasselmann (1976) theory in the absence of resonant eigenoscillations which would introduce additional peaks in the autospectra. Thus, in marked contrast to the situation in the tropics where the surface heat flux acts as a negative feedback on the SST to first order, variations in surface heat flux drive the SST in the north Atlantic.

6. Conclusions

We have performed a twenty year integration with our global coupled ocean-atmosphere general circulation model "ECHO". Flux correction was not applied to couple the individual model components. Climate drift is appreciably small but still significant. The coupled model simulates considerable interannual variability in the tropics and in mid-latitudes, with spatial patterns similar to those observed. The variance of the tropical variability is somewhat underestimated, while the level of variability in mid-latitudes is simulated realistically.

ECHO is a coupled model of the latest generation. Such coupled GCMs are being currently developed by several groups worldwide. These models have reached a level of sophistication which no longer requires the application of flux correction techniques. Climate "crashes" or climate "catastrophes" do not occur in these models, as was often the case in the past (the reader is referred for a discussion of climate drift in coupled models to the review article by Neelin et al. (1992)). Coupled GCMs will be used to study the nature of air–sea interactions, especially in regions where not enough data are available, and they will be applied more and more to the issue of short-range climate forecasting.

However, despite these encouraging aspects, coupled GCMs have still serious problems. As described in this paper, the parameterization of certain physical processes must be improved considerably. Examples are, for instance, the representation of clouds and of oceanic mixing processes. Coupled GCMs form a useful framework for testing such parameterizations, since they are less constrained than uncoupled models. In the next step, we shall couple a sophisticated sea ice model (Hibler, 1979) to ECHO, in order to be able to resolve the full variability spectrum on the short-range climatic time scale up to a decade. The simulation of sea ice is a delicate issue, as past experiences with coupled models show (Cubasch et al., 1994).

7. Acknowledgements

We like to thank Professor Dr. Klaus Hasselmann for many fruitful discussions. This work was supported by the Koerber project and by the European Community under grant no. EV5V-CT92-0121. The coupled integations were performed at the Deutsches Klimarechenzentrum (DKRZ) which is sponsored by the Bundesministerium für Forschung und Technologie and other agencies.

REFERENCES

Alexander, M. A. 1990. Simulation of the response of the North Pacific Ocean to the anomalous atmospheric circulation associated with El Niño. *Climate Dynamics* **5**, 53–65.

Arpe, K. and Dümenil, L. 1993. *Validation of the ECHAM model with respect to precipitation, snow and river runoff.* WMO/TD-No. 544, 107–112. Available from World Meteorological Organization, Case postale No. 2300, CH-1211 Geneva 20, Switzerland.

Barnett, T. P., Latif, M., Kirk, E. and Roeckner, E. 1991. On ENSO physics. *J. Climate* **4**, 487–515.

Barnston, A. G. and Livezey, R. E. 1987. Classification, seasonality, and persistence of low-frequency atmospheric circulation patterns. *Mon. Wea. Rev.* **115**, 1083–1126.

Cayan, D. 1992. Latent and sensible heat flux anomalies over the Northern Oceans: Driving the sea surface temperature. *J. Phys. Oceanogr.* **22**, 859–881.

Cubasch, U., Hasselmann, K., Höck, H., Maier-Reimer, E., Mikolajewicz, U., Santer, B. D. and Sausen, R. 1992. Time-dependent greenhouse warming computations with a coupled ocean-atmosphere model. *Climate Dynamics* **8**, 55–69.

Cubasch, U., Santer, B. D., Hellbach, A., Hegerl, G., Höck, H., Maier-Reimer, E., Mikolajewicz, U., Stössel, A. and Voss, R. 1994. Monte Carlo climate change forecasts with a global coupled ocean-atmosphere model. *Climate Dynamics*, in press.

Delworth, T., Manabe, S. and Stouffer, R. J. 1993. Interdecadal variability of the thermohaline circulation in a coupled ocean-atmosphere model. *J. Climate* **6**, 1993–2011.

DKRZ, 1992. *The ECHAM 3 atmospheric general circulation model.* Deutsches Klimarechenzentrum, report no. 6. Available from Deutsches Klimarechenzentrum, Bundesstr. 55, D-20146 Hamburg, Germany.

Fischer, G. 1987. *Large-scale atmospheric modeling*, report no. 1. Meteorological Institute, University of Hamburg, Germany. Available from Meteorologisches Institut der Universität Hamburg, Bundesstr. 55, D-20146 Hamburg, Germany.

Gill, A. E. 1982. *Atmosphere-ocean dynamics.* Academic Press.

Gordon, C. 1989. Tropical ocean-atmosphere interactions in a coupled model. *Phil. Trans. Roy. Soc. Lond.* **A329**, 207–223.

Hasselmann, K. 1976. Stochastic climate models. Part I: Theory. *Tellus* **28**, 473–485.

Hibler, W. D., III, 1979. A dynamic thermodynamic sea ice model. *J. Phys. Oceanogr.* **9**, 815–846.

Jager, L. 1976. Monatskarten des Niederschlages für die ganze Erde. *Berichte des Deutschen Wetterdienstes* **139**, 1–38.

Latif, M. 1987. Tropical ocean circulation experiments. *J. Phys. Oceanogr.* **17**, 246–263.

Latif, M., Biercamp, J., Von Storch, H., McPhaden, M. J. and Krik, E. 1990. Simulation of ENSO related surface wind anomalies with an atmospheric GCM forced by observed SST. *J. Climate* **3**, 509–521.

Latif, M., Sterl, A., Maier-Reimer, E. and Junge, M. M. 1993a. Climate variability in a coupled GCM. Part I: The tropical Pacific. *J. Climate* **6**, 5–21.

Latif, M., Sterl, A., Maier-Reimer, E. and Junge, M. M. 1993b. Structure and predictability of the El Niño/Southern Oscillation phenomenon in a coupled ocean-atmosphere general circulation model. *J. Climate* **6**, 700–708.

Lau, N.-C., Philander, S. G. H. and Nath, M. J. 1992. Simulation of El Niño/Southern Oscillation phenomena with a low-resolution coupled general circulation model of the global ocean and atmosphere. *J. Climate* **5**, 284–307.

Legates, D. R. and Willmott, C. J. 1990. Mean seasonal and spatial variability in gauge corrected global precipitation. *J. Climatology* **10**, 111–127.

Levitus, S. 1982. *Climatological atlas of the worlds ocean.* NOAA Prof. Paper no. 13, U.S. Govt. Printing Office, Washington DC, 173 pp., 17 microfiche.

Luksch, U. and Von Storch, H. 1992. Moedling the low-frequency sea surface temperature variability in the North Pacific. *J. Climate* **5**, 893–906.

Manabe, S., Bryan, K. and Spelman, M. J. 1990. Transient response of a global ocean-atmosphere model to a doubling of atmospheric carbon dioxide. *J. Phys. Oceanogr.* **20**, 722–749.

Meehl, G. A. 1990. Seasonal cycle forcing of El Niño-Southern Oscillation in a global coupled ocean-atmosphere GCM. *J. Climate* **3**, 72–98.

Murphy, J. M. 1990. Transient response of climate to a gradual increase in CO_2, using a coupled ocean/atmosphere model with flux correction. In: *Research activities in atmospheric and oceanic modeling*, G. Boer (ed.). WMO/TD-No. 396.

Nagai, T., Tokioka, T., Endoh, M. and Kitamura, Y. 1992. El Niño-Southern Oscillation simulated in an MRI atmosphere-ocean coupled general circulation model. *J. Climate* **5**, 1202–1233.

Neelin, J. D., Latif, M., Allaart, M. A. F., Cane, M. A., Cubasch, U., Gates, W. L., Gent, P. R., Ghil, M., Gordon, C., Lau, N. C., Mechoso, C. R., Meehl, G. A., Oberhuber, J. M., Philander, S. G. H., Schopf, P. S., Sperber, K. R., Sterl, A., Tokioka, T., Tribbia, J. and Zebiak, S. E. 1992. Tropical air–sea interaction in general circulation models. *Climate Dynamics* **7**, 73–104.

Oberhuber, J. M. 1988a. *An atlas based on the "COADS" data set: Fields of mean wind, cloudiness and humidity at the surface of the global ocean.* Max-Planck-Institut für Meteorologie, report no. 14.

Oberhuber, J. M. 1988b. *An atlas based on the "COADS" data set: The budgets of heat, buoyancy and turbulent*

kinetic energy at the surface of the global ocean. Max-Planck-Institut für Meteorologie, report no. 15.

Paulson, C. A. and Simpson, J. J. 1977. Irradiance measurements in the upper ocean. *J. Phys. Oceanogr.* **7**, 952–956.

Philander, S. G. H., Pacanowski, R. C., Lau, N.-C. and Nath, M. J. 1992. Simulation of ENSO with a global atmospheric GCM coupled to a high-resolution, tropical Pacific ocean GCM. *J. Climate* **5**, 308–329.

Reynolds, W. R. 1988. A real-time global sea surface temperature analysis. *J. Climate* **1**, 75–86.

Roeckner, E., Arpe, K., Bengtsson, L., Brinkop, S., Dümenil, L., Esch, M., Kirk, E., Lunkeit, F., Ponater, M., Rockel, B., Sausen, R., Schlese, U., Schubert, S. and Windelband, M. 1992. *Simulation of the present-day climate with the ECHAM model: impact of model physics and resolution.* Max-Planck-Institut für Meteorologie, report no. 93. Available from Max-Planck-Institut für Meteorologie, Bundesstr. 55, D-20146 Hamburg, Germany.

Sausen, R., Barthel, K. and Hasselmann, K. 1988. Coupled ocean-atmosphere models with flux correction. *Climate Dynamics* **2**, 154–163.

Schopf, P. S. and Suarez, M. J. 1988. Vacillations in a coupled ocean-atmosphere model. *J. Atmos. Sci.* **45**, 549–566.

Shea, D. 1986. *Climatological atlas: 1950–1979.* Atmospheric Analysis and Prediction Divison. National Center for Atmospheric Research, Boulder Colorado, USA.

Stockdale, T., Burgers, G., Latif, M. and Wolff, J. 1994. Some sensitivities of a coupled ocean-atmosphere GCM. *Tellus* **46A**, 367–380.

Von Storch, H. 1988. *Large-scale atmospheric modeling.* Report no. 4, Meteorological Institute, University of Hamburg, Germany. Available from Meteorologisches Institut der Universität Hamburg, Bundesstr. 55, D-20146 Hamburg, Germany.

Wallace, J. M. and Gutzler, D. S. 1981. Teleconnections in the geopotential height field during northern hemipshere winter. *Mon. Wea. Rev.* **109**, 784–812.

Washinngton, W. M. and Meehl, G. A. 1989. Climate sensitivity due to invreased CO_2: Experiments with a coupled atmosphere ocean general circulation model. *Climate Dynamics* **4**, 1–38.

Weare, B. C., Navato, A. R. and Newell, R. E. 1976. Empirical orthogonal analysis of Pacific sea surface temperature. *J. Phys. Oceanogr.* **6**, 671–678.

Wolff, J. and Maier-Reimer, E. 1993. HOPE: *The Hamburg primitive equation ocean model.* Deutsches Klimarechenzentrum, Technical Report, in press.

Zorita, E., Kharin, V. and Von Storch, H. 1992. The atmospheric circulation and sea surface temperature in the north Atlantic area in winter. Their interaction and relevance for Iberian precipitation. *J. Climate* **5**, 1097–1108.